Synthesis and optical properties of 1-ethyl-indol-3-yl-substituted aza-BODIPY dyes at the 1,7-positions

Luis Loaeza, Ricardo Corona-Sánchez, Geraldyne Castro, Margarita Romero-Ávila, Rosa Santillan, Valérie Maraval, Rémi Chauvin, Norberto Farfán

Synthesis and optical properties of 1-ethyl-indol-3-yl-substituted aza-BODIPY dyes at the 1,7-positions

Luis Loaeza,[a,c] Ricardo Corona-Sánchez,[a,d] Geraldyne Castro,[a] Margarita Romero-Ávila,[a] Rosa Santillan,[b] Valérie Maraval,[c] Remi Chauvin,[c*] and Norberto Farfán[a*]

[a]Facultad de Química, Departamento de Química Orgánica, Universidad Nacional Autónoma de México, 04510 Ciudad de México, México.

[b]Departamento de Química, Centro de Investigación y de Estudios Avanzados del IPN, Apdo. Postal 14-740, 07000 Ciudad de México, México.

[c]LCC-CNRS, Université de Toulouse, CNRS, UPS, Toulouse, France.

[d]Departamento de Química, Universidad Autónoma Metropolitana-Iztapalapa, Av. San Rafael Atlixco 186, Leyes de Reforma 1ra Secc., 09340 Ciudad de México, México.

*Corresponding authors e-mail address: N. F. norberto.farfan@gmail.com
R. C. chauvin@lcc-toulouse.fr

Keywords:
Aza-BODIPY
Indol-3-yl substituents
Near-infrared
Bathochromic shift

Abstract

New aza-BODIPYs with significant bathochromic shifts in their UV-vis absorption spectrum were synthesized by the installation of 1-ethyl-indol-3-yl moieties at the 1,7-positions of the aza-BODIPY core bearing 4-substituted phenyl or thien-2-yl groups at the 3,5-positions. The compounds described herein show strong NIR absorptions up to 779 nm, and emissions up to 805 nm in chloroform solution, and present large molar extinction coefficients. The absorption and emission bands of aza–BODIPYs were significantly red-shifted, by *ca* 100 nm, relative to the 3,5-dianisyl-1,7-diphenyl aza-BODIPY. TD-DFT calculation indicate an effective electronic conjugation between the aza-BODIPY core and the substituents. Absorption of the aza-BODIPYs corresponds to a charge transfer from donor substituents toward the boron-centered core. Moreover, these computational results show that all the compounds present HOMO–LUMO band gap values that are in the organic semiconductor range.

1. Introduction

In recent years, the interest in molecules absorbing and emitting in the near-infrared region (NIR) has increased, especially for the purpose of medicine and materials science. In the domain of medicine, the region between 700 and 1100 nm, denominated the "biological window", is attractive for numerous biological applications because in this range of wavelength the light has deep tissue penetration and does not damage living tissues.[1] In materials science, wavelengths extending in the NIR region are particularly important for optoelectronic applications. Indeed, about 51% of solar energy falls in the near-infrared region,[2] calling for the development of new dyes and materials absorbing in this region to increase the efficiency in solar energy conversion (e.g. by organic photovoltaic solar cells or water-splitting photocatalysts[3]). Amongst the large variety of NIR chromophores, aza-BODIPY dyes have attracted significant attention due to their remarkable photophysical properties such as tunable absorption and emission wavelengths, high photostability, and large molar absorption coefficients.[4] These characteristics make them promising candidates for potential applications, e.g. in bioimaging,[5] photodynamic therapy,[6] sensing,[7] optoelectronics,[8] and general nonlinear optics.[9]

Taking as reference the 1,3,5,7-tetraphenyl-aza-BODIPY which absorbs at 650 nm and emits at 672 nm in chloroform,[10] several structural modifications have been reported to shift the absorption and emission bands further to the NIR range. These approaches include the substitution by electron-donating groups[9,11] -or both electron-donating and electron-withdrawing groups-[12] on the phenyl rings, rigidification of rotatable moieties,[13] extension of the π-conjugation,[14] benzannulation of the pyrrole ring,[15] formation of intramolecular B–O six-membered rings,[16] and reduction of the torsion angles by replacing phenyl substituents by thienyls.[17] Nevertheless, one of the most popular general strategy to modify the optical properties of π-conjugated molecules consists in the introduction of resonating donor (D) and acceptor (A) motifs to form push-pull systems.[18] This approach applied to aza-BODIPYs has proven to contribute significantly to a bathochromic shift of their absorption to the NIR region, as, for example, in 1,7-difluorophore-substituted aza-BODIPYs in which a naphthalene, pyrene, or *N*-substituted carbazole group operates as the donor unit and the aza-BODIPY core as the acceptor fragment.[19]

A large variety of aza-BODIPYs with diverse substituents at the 1,7-positions was reported, but to our knowledge, strongly electron-donating 3-indolyl moieties[20] have not been envisaged at those positions yet, though it has been shown that such motifs at the 2,6-positions improve the optical properties of aza-BODIPYs.[21] Therefore, in this work, 1-ethyl-indol-3-yl substituents were introduced in the 1,7-positions with different substituents at the 3,5-positions of the aza-BODIPY core (Figure 1), with the view to studying their effect on the photophysical properties of the obtained chromophores. These 1-ethyl-indol-3-yl-substituted aza-BODIPYs are shown to exhibit red-shifted absorption and emission maxima. Additionally, TD-DFT computational studies were carried out to present a complementary spectroscopic insight with the purpose of estimating the wavelength of maximum absorption of this type of dyes.

Reported structure

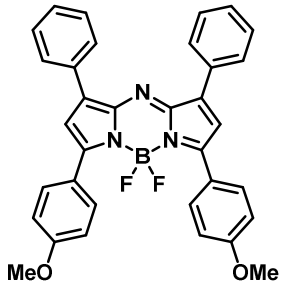

4aPh

λ_{abs} = 688 nm
λ_{em} = 715 nm

This work

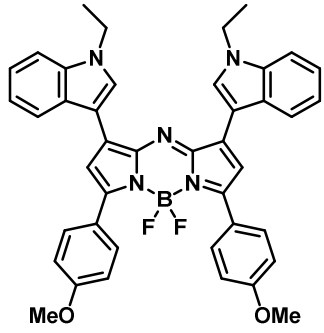

4a

λ_{abs} = 750 nm
λ_{em} = 781 nm

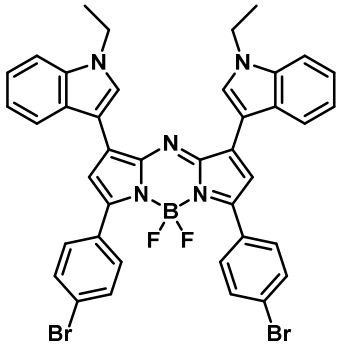

4b

λ_{abs} = 768 nm
λ_{em} = 804 nm

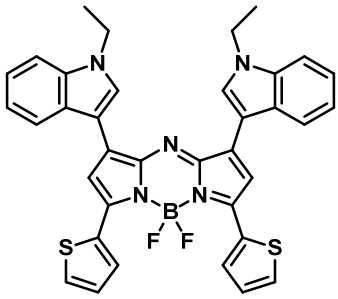

4c

λ_{abs} = 779 nm
λ_{em} = 805 nm

Figure 1. Aza-BODIPYs **4a–4c** reported in this work (data in chloroform).

2. Results and Discussion

2.1. Synthesis and Characterization

The synthesis of the target compounds **4a–c** (Scheme 1) was performed using the O'Shea approach.[9,22] This strategy involves the formation of the α,β-unsaturated ketones **1a–c** by an aldol condensation reaction using one equivalent of 1-ethylindole-3-carboxaldehyde and one equivalent of the selected methylketone in the presence of KOH. The enones **1a–c** were found to precipitate as yellow solids in 84–89% yields. Then, the 1,3-diaryl-4-nitrobutan-1-ones **2a–c** were synthesized in 80–85% yields *via* a 1,4 Michael addition reaction of nitromethane to the corresponding α,β-unsaturated ketones **1a-c**. The obtained adducts **2a-c** were subsequently treated with an excess of ammonium acetate in butanol to give the aza-dipyrromethenes **3a–c** in 25–34% yields. Finally, the the aza-BODIPYs **4a–c** were obtained by reaction of the corresponding aza-dipyrromethene with $BF_3{\cdot}Et_2O$ in the presence of triethylamine. The targeted aza-BODIPYs **4a-c** were isolated as dark blue-violet solids in 79–88% yields.

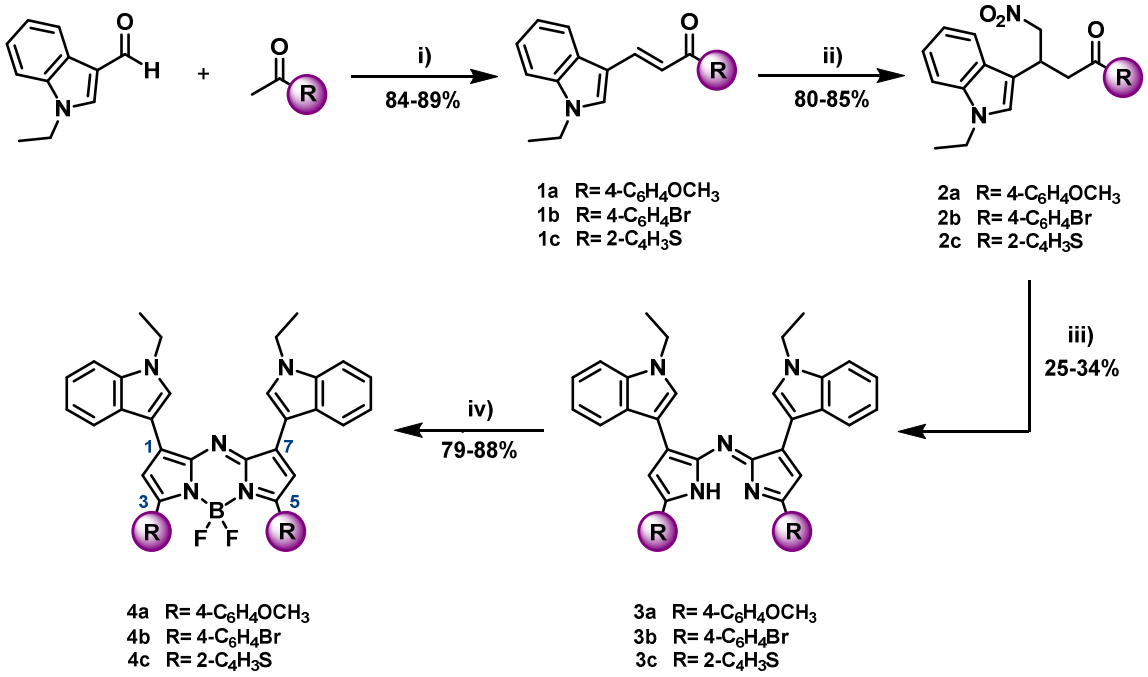

Scheme 1. Synthesis of 1-ethyl-indol-3-yl-substituted aza-BODIPYs **4a–c**. (i) KOH, EtOH, rt, (ii) CH_3NO_2, MeOH/NEt_3, reflux, (iii) NH_4OAc, BuOH, reflux, (iv) NEt_3, $BF_3{\cdot}Et_2O$, CH_2Cl_2, reflux

All the intermediates (**1a–c**, **2a–c**, **3a–c**), and final products **4a–c** were characterized by HRMS, ^1H, and ^{13}C NMR spectroscopy. The characteristic β-pyrrole protons for **4a–c** appeared as singlet signals around 7.00 ppm, while the α-1-ethylindole protons gave a singlet signal around 8.05 ppm (see the supplementary data). The aliphatic protons appeared as quartet and a triplet signals at 4.20 ppm and 1.46 ppm, respectively. The aza-BODIPYs **4a–c** were also characterized by ^{19}F and ^{11}B NMR spectroscopy in CD_2Cl_2 solution (Table 1). These compounds showed a typical quartet ^{19}F NMR signal and a triplet ^{11}B NMR signal due to ^{11}B–^{19}F coupling. The ^{19}F signals appeared between -129.44 ppm and -135.82 ppm, while ^{11}B signals appeared between 1.00 ppm and 1.27 ppm. Particularly, the ^{11}B chemical shift value of the thienyl substituted aza-BODIPY **4c** was found slightly high frequency shifted, compared to **4a** and **4b** as a result of an increased delocalization of electronic density in the aza-BODIPY core of **4c**. The 3,5-dianisyl-1,7-diphenyl aza-BODIPY **4aPh** was also prepared according to a literature protocol[9] and was used to compare their optical properties *versus* the compounds **4a–c**.

Table 1. ^{19}F and ^{11}B NMR chemical shift values recorded in CD_2Cl_2

Compound	^{19}F signal (δ/ppm)	^{11}B signal (δ/ppm)
4aPh	-131.76	0.06
4a	-130.11	1.16
4b	-129.44	1.00
4c	-135.82	1.27

2.2. Spectroscopic characteristics

The optical properties of the aza-BODIPYs **4a–c** were evaluated in three solvents with different polarities: tetrahydrofuran, chloroform, and toluene. The three dyes **4a–c** present absorption and emission in the NIR region with large molar extinction coefficients. The values of the wavelength of maximum absorption, emission, molar extinction coefficients, and relevant photophysical data are listed in Table 2, and compared to those of the selected 3,5-dianisyl-1,7-diphenyl-aza-BODIPY reference **4aPh**.[9]

Table 2. Optical properties of aza-BODIPYs **4a–c** in different solvents

Compound	Solvent (β, E_T^N)[a]	λ_{abs}, ε (nm, M^{-1} cm^{-1})	$Fwhm_{abs}$[b] (nm)	λ_{em} (nm)	$Fwhm_{em}$[b] (nm)	Stokes shift (nm)
4aPh	$CHCl_3$ (0.10, 0.26)	688 (85 000)[c]	55[c]	715[c]	–	27[c]
4a	THF (0.55, 0.21)	601 (25 800), 753 (57 100)	93	783	68	30
	$CHCl_3$ (0.10, 0.26)	598 (22 800), 750 (52 700)	92	781	67	31
	Toluene (0.11, 0.10)	596 (20 400), 749 (51 700)	88	771	60	22
4b	THF (0.55, 0.21)	615 (32 800), 777 (43 000)	117	813	52	36
	$CHCl_3$ (0.10, 0.26)	610 (35 600), 768 (48 400)	116	804	59	36
	Toluene (0.11, 0.10)	609 (13 200), 767 (20 900)	110	796	62	29
4c	THF (0.55, 0.21)	621 (18 800), 782 (44 100)	88	807	59	25
	$CHCl_3$ (0.10, 0.26)	616 (18 600), 779 (50 400)	77	805	57	26
	Toluene (0.11, 0.10)	615 (23 400), 780 (63 500)	71	800	55	20

[a] β = Kamlet-Taft solvent basicity parameter, E_T^N = solvent polarity parameter normalized *vs* tetramethylsilane (0.00) and water (1.00).[23]
[b] $Fwhm_{abs}$, $Fwhm_{em}$: full-width at half-maximum.
[c] Data from the literature.[9]

The aza-BODIPYs **4–c** show a dual absorption profile that extends from 500 to 850 nm (Figure 2, Table 2). The maximum absorption band located at 750 nm for **4a**, 768 nm for **4b**, and 779 nm for **4c** in chloroform solutions is attributed to the $S_0 \rightarrow S_1$ transition. The corresponding absorption coefficients are in the range of 48 400–52 700 M^{-1} cm^{-1}. A second absorption band with medium intensity is observed in the 500–650 nm region (ε = 18 600–35 600 M^{-1} cm^{-1}) and should correspond to the $S_0 \rightarrow S_2$ transition, being particularly intense for the dye **4c**. Furthermore, the less-intense band around 300–400 nm can be assigned to the 1-ethyl-indol-3-yl moieties. The data in Table 2 show that the 1-ethyl-indol-3-yl substituents in **4a** induced a 62 nm red-shift of the maximum absorption wavelength as compared to the phenyl substituents in the reference aza-BODIPY **4aPh** (λ_{abs} = 688 nm in chloroform).[9] This is attributed to the electron-donating effect of the 1-ethyl-indol-3-yl moiety. The maximum absorption wavelength of the 3,5-dithienyl-

substituted aza-BODIPY **4c** is red-shifted by 29 and 11 nm in comparison with 3,5-diaryl-substituted counterparts **4a** and **4b**, respectively. This significant bathochromic shift for **4c** can be attributed to the smaller torsion angles between the pyrrole ring plane and the thienyl ring plane, *versus* 4-substituted phenyl ring planes. As observed in Table 2, the absorption wavelengths of the aza-BODIPYs **4a–c** are only slightly solvent-dependent. For example, upon increasing the polarity of the solvent from toluene to THF, the most noticeable solvatochromic effect was observed for **4b**, bearing the less electron-donating group (C_6H_4Br), with a 10 nm bathochromic shift of the maximum absorption band. A systematic trend for all the compounds is a slight increase of the λ_{abs} value through the sequence toluene ≈ chloroform < THF, i.e. through increasing solvent Lewis basicity as quantified by the Kamlet-Taft parameter β, suggesting a possible stabilization of the most polar zwitterionic valence bond form of the aza-BODIPY by interaction of [23]the THF oxygen lone pair with the indolium moiety (Et-N=CH^+<–:$O(C_2H_4)_2$). However, the full-width at half-maximum of absorption ($Fwhm_{abs}$) of the main absorption band is also broader for **4b** (around 114 nm) than for **4a** and **4c** in all the solvents.

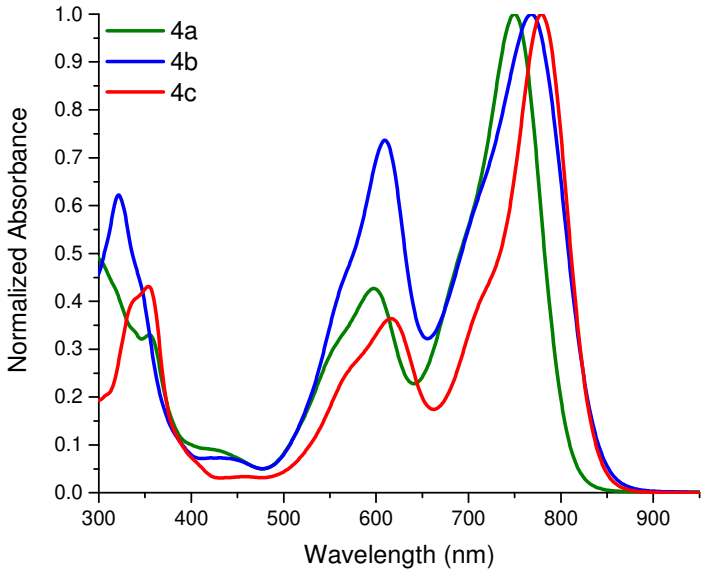

Figure 2. Normalized absorption spectra of the aza-BODIPYs **4a-c** in chloroform

Excitation of the aza-BODIPYs **4a–c** at 700 nm induces emission in the range 771–813 nm depending on the solvent (Table 2). In chloroform solution, the emission bands of **4a-c** are localized between 781 and 805 nm (Figure 3). In this solvent, the wavelength of maximum emission of the 3,5-dithienyl-substituted aza-BODIPY **4c** is red-shifted by 90 nm as compared to the reference aza-BODIPY **4aPh** (λ_{em} = 715 nm in chloroform),[9] but only by 24 nm *vs* **4a** and 1 nm *vs* **4b**. Solvatochromism studies revealed that the emission wavelengths of aza-BODIPYs **4a–c** are only slightly solvent-dependent, with small shifts of 2–12 nm for **4a**, 8–17 nm for **4b**, and 2–7 nm for **4c**, the most notable solvatochromic effect of 17 nm being observed for **4b** when changing the solvent from tetrahydrofuran to toluene. The largest Stokes shift of 36 nm occurs for **4b** in polar solvents (tetrahydrofuran and chloroform). For the three compounds a marked systematic solvent

effect is observed for the Stoke shift: 5-8 nm greater in THF and chloroform than in toluene (thus grossly correlating with the normalized solvent polarity parameter E_T^N).[23] It is finally noteworthy that the aza-BODIPY **4a** exhibits the broadest full-width half-maximum of emission ($Fwhm_{em}$) around 65 nm in all the solvents.

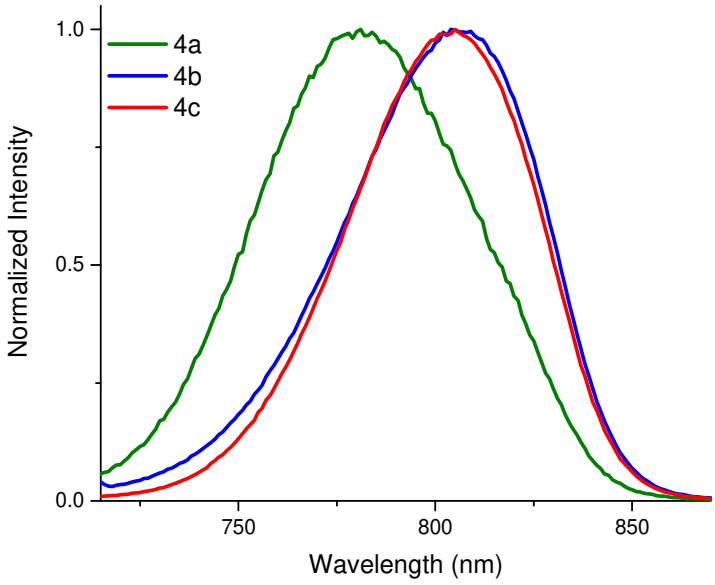

Figure 3. Normalized emission spectra of the aza-BODIPYs **4a-c** in chloroform

2.3. Computational Methodology

To elucidate the origin of the optical properties in aza-BODIPYs **4a–c**, computational calculations were performed with a standard protocol reported in the literature for aza-BODIPY dyes.[24] The ground state geometries of **4a–c** were optimized at the PBE0/6-311G(2d,p) level of theory, followed by calculation of the harmonic vibrational frequencies to ascertain that the optimized geometries correspond to minima of energy. The electronic transitions were calculated for the optimized geometries at the TD-DFT/BMK/6-311+G(2d,p) level of approximation. The solvation by chloroform has been estimated in the calculations under the PCM model. All the calculations were performed using Gaussian 09 and the GaussView 5.0 visualization suite.[25]

The calculated dihedral angles (Table 3) between the thienyl ring planes and the mean plane of the aza-BODIPY core of **4c** (φ = 26°) are smaller, thus improving the molecular planarity in comparison with the 4-substituted phenyl derivatives (φ = 37° for **4a** and φ = 39° for **4b**). The dihedral angles between the indolyl planes and the mean plane of the aza-BODIPY core are calculated to be much lower at 17.7 ± 0.5°, the steric hindrance being smaller on this "north" side of the aza-BODIPY core.

The contour plots of the frontier molecular orbitals (FMOs) for the aza-BODIPYs **4a–c** are presented in Figure 4. Considering the TD-DFT calculated excited states, the wavelength of maximum absorption of **4a** exclusively accounts for a HOMO→LUMO electronic promotion, whereas those of **4b** and **4c** corresponds to a combination of HOMO→LUMO and HOMO-1→LUMO excitations with a dominance of the former. The delocalization of the FMOs is a consequence of an effective electronic conjugation between the aza-BODIPY core and substituents through the 1,3,5,7-positions. Likewise, the TD-DFT calculations indicate that for all the dyes **4a–c**, the absorptions in the visible range correspond to charge transfers from the substituents to the central aza-BODIPY core. Due to similar topologies of the LUMO in molecules **4a–c**, it is observed that the aza–BODIPY core acts as a strong accepting unit and the 1-ethyl-indol-3-yl substituent as a strong donating unit.

The $\lambda_{abs\ max}$ values calculated for **4a–c** are presented in Table 4 and compared to the experimental values. These absorption wavelengths reflect the HOMO–LUMO gap, as evidenced by the TD-DFT studies. The calculated $\lambda_{abs\ max}$ value was underestimated by 9 nm for **4a**, 54 nm for **4b**, and 42 nm for **4c** as compared to the experimental data, but remains in quite good agreement. The calculated HOMO and LUMO orbital energy levels, and the values of the HOMO–LUMO gaps are given in Table 4. The HOMO and LUMO eigenvalues of the aza-BODIPYs **4a–c** are located between the HOMO and LUMO eigenvalues of PCBM (HOMO = –6.0 eV, LUMO = –4.3 eV) and P3HT (HOMO = –5.1 eV, LUMO = –2.9 eV), thus making diindolyl-aza-BODIPYs potential candidates for the elaboration of ternary inverted organic solar cells.[7b] The HOMO–LUMO optical gaps of **4a–c** were also calculated from the absorption onset in the UV-Vis studies, and were found to be quite low, between 1.48 and 1.53 eV.

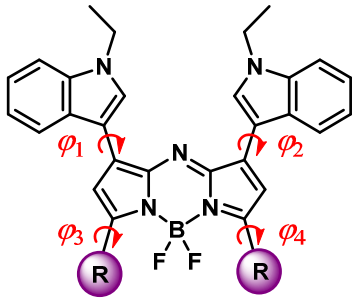

Table 3. Computed values of the torsion angles (in degrees) defining the tilt of the substituents with respect to the aza-BODIPY core plane.

Compound	φ_1	φ_2	φ_3	φ_4
4a	18	17	37	37
4b	18	17	39	39
4c	18	17	26	26

Table 4. Energies of the HOMO and the LUMO, HOMO–LUMO gaps, and comparison between TD-DFT-computed and experimental $\lambda_{abs\ max}$ values.

Compound	HOMO[a] (eV)	LUMO[a] (eV)	$E_{(H\text{-}L)}$[a] (eV)	$E_{(H\text{-}L)}$[b] optical (eV)	$\lambda_{abs\ max}$[c] (nm) (f)	$\lambda_{abs\ max}$[d] (nm)

4a	-5.72	-3.74	1.98	1.53	741 (0.35)	750
4b	-5.89	-3.88	2.01	1.48	714 (0.42)	768
4c	-5.78	-3.83	1.95	1.49	737 (0.36)	779

[a] Calculated with PBE0/6-311G(2d,p) level of theory.

[b] Optical band gap estimated from the onset wavelength of the UV–Vis spectra in $CHCl_3$.

[c] Calculated with TD-DFT/BMK/6-311+G(2d,p) level of theory. *f* = oscillator strength.

[d] Experimental maximum absorption wavelength in $CHCl_3$.

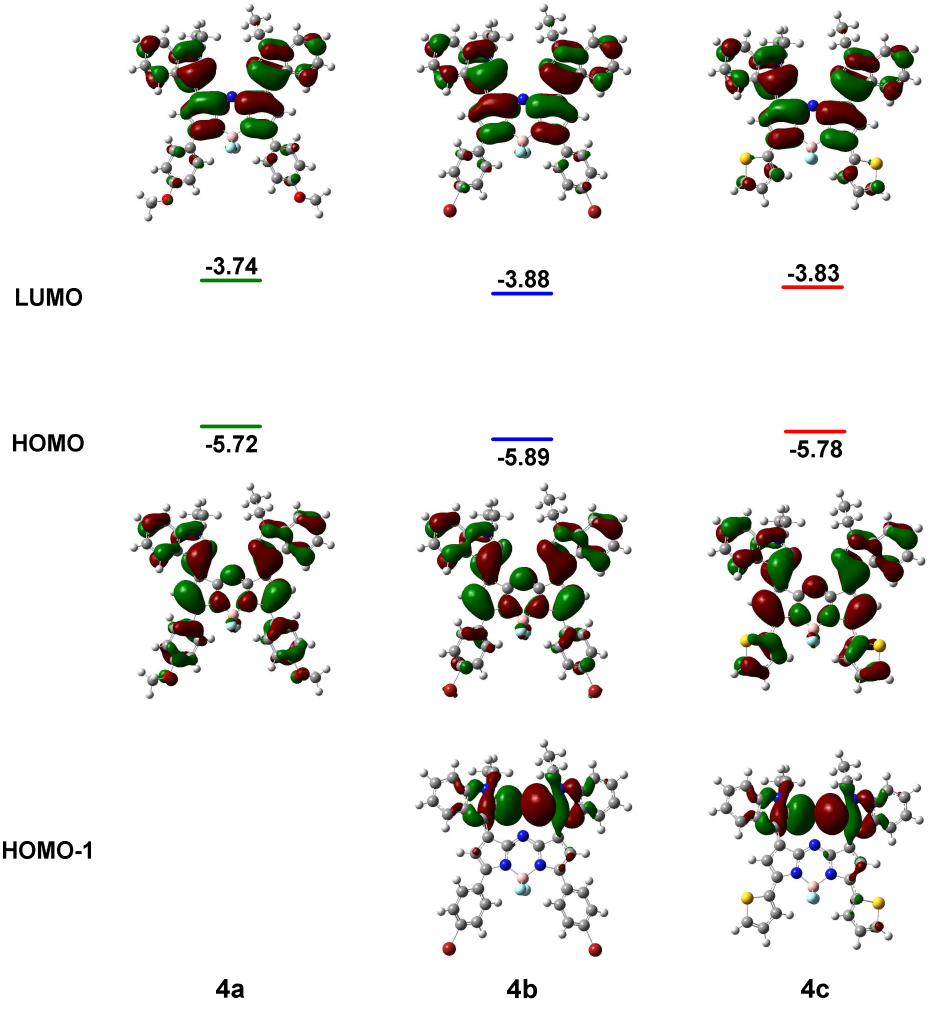

Figure 4. Contour plots of the frontier molecular orbitals for the aza-BODIPYs **4a-c** (PBE0/6-311G(2d,p))

3. Conclusion

The synthesis, absorption and emission properties of unprecedented aza-BODIPYs bearing 1-ethyl-indol-3-yl substituents as donating motifs at the 1,7-positions and 4-substituted phenyl and thien-

2-yl rings at the 3,5-positions, have been disclosed. By comparison with the 3,5-dianisyl-1,7-diphenyl-aza-BODIPY reference, the absorption and emission bands are shifted to the near-infrared region thanks to the 1-ethyl-indol-3-yl moieties, in agreement with their strong electron-donating character. The introduction of such electron-rich fluorophores at the 1,7-positions thus appears to be a simple method to shift the absorption and emission bands to the NIR range, by avoiding "π-frustration"[26] through the electron-accepting and dipolar character of the aza-BODIPY core. Furthermore, the thienyl groups were shown to develop stronger electronic interactions with the aza-BODIPY core than the 4-substituted phenyl counterparts, and thus to induce a redshift of the corresponding electronic spectra. TD-DFT studies allowed a detailed analysis of the effective electronic interactions between the donor periphery and the acceptor core in all the synthesized 1-ethyl-indol-3-yl- aza-BODIPY derivatives. DFT-calculated HOMO–LUMO band gap values are found to lie in the organic semiconductor range, thus opening prospects of applications in organic photovoltaics.

4. Experimental Section

4.1. Materials, solvents and instrumentation

All starting materials were purchased from Aldrich and used without further purification, except for 1-ethylindole-3-carboxaldehyde that was synthesized according to a literature protocol.[27] Solvents were dried using standard methods or distilled prior to use. Reactions were monitored by TLC on precoated silica gel plates (Aldrich Silica gel on TLC plates with fluorescent indicator 254 nm) and revealed by exposure to a UV lamp.

^{1}H, ^{13}C, ^{19}F, and ^{11}B NMR spectra were recorded using a Bruker 400 spectrometer. Chemical shifts (δ/ppm) are reported relative to $Si(CH_3)_4$, $CDCl_3$, or CD_2Cl_2.

FT-IR spectra were measured on a PerkinElmer Frontier FT-IR spectrophotometer.

High-resolution mass spectrometry was acquired using an Agilent Technologies ESI-TOF spectrometer.

Experimental UV-visible spectra were determined using a Thermo Scientific Evolution 220 spectrophotometer.

Experimental emission spectra were recorded using a FluoroMax-4 spectrofluorometer.

4.2. Synthesis

*4.2.1. General procedure for α,β-unsaturated ketones (**1a–c**)*

A mixture of 1-ethylindole-3-carboxaldehyde (1 equivalent, 8.66 mmol) and the corresponding methylketone (1 equivalent, 8.66 mmol) in ethanol (20 mL) was treated with KOH (2.5 equivalents, 21.65 mmol). During the course of the reaction, the product precipitated from the reaction mixture. The precipitate was filtered and washed with water. The products were purified through column chromatography on silica gel using a *n*-hexane/acetone eluting mixture.

4.2.1.1. **Compound 1a**. The product was obtained as a yellow solid in 89% yield. Melting point: 112–113 °C. ^{1}H-NMR (400.16 MHz, $CDCl_3$, δ/ppm): 8.14 – 8.05 (m, 3H), 8.04 – 8.00 (m, 1H), 7.57 (d, *J* = 15.5 Hz, 1H), 7.51 (s, 1H), 7.43 – 7.37 (m, 1H), 7.35 – 7.28 (m, 2H), 7.04 – 6.94 (m, 2H), 4.19 (q, *J* = 7.3 Hz, 2H), 3.89 (s, 3H), 1.51 (t, *J* = 7.3 Hz, 3H). ^{13}C-NMR (100.63 MHz, $CDCl_3$, δ/ppm): 189.0, 163.0, 138.0, 137.3, 132.7, 132.0, 130.5, 126.4, 123.0, 121.5, 120.9, 116.7, 113.7, 113.1, 110.2, 55.5, 41.5, 15.3. FT-IR (ATR, cm^{-1}): 3093, 1648, 1597, 1583, 1559, 1372, 1257, 1213, 1161, 1026, 813, 727, 594. ESI-TOF HRMS for $C_{20}H_{20}NO_2$ calculated: 306.1488, found: $[M + H]^+$ 306.1488.

4.2.1.2. **Compound 1b**. The product was obtained as a yellow solid in 84% yield. Melting point: 136–137 °C. ^{1}H-NMR (400.16 MHz, $CDCl_3$, δ/ppm): 8.10 (d, *J* = 15.5 Hz, 1H), 8.03 – 7.98 (m, 1H), 7.95 – 7.90 (m, 2H), 7.67 – 7.62 (m, 2H), 7.56 (s, 1H), 7.48 (d, *J* = 15.5 Hz, 1H), 7.43 – 7.40 (m, 1H), 7.37 – 7.29 (m, 2H), 4.23 (q, *J* = 7.3 Hz, 2H), 1.54 (t, *J* = 7.3 Hz, 3H). ^{13}C-NMR (100.63 MHz, $CDCl_3$, δ/ppm): 189.6, 139.5, 137.5, 138.1, 133.3, 131.9, 130.0, 127.1, 126.4, 123.3, 121.8, 121.0, 116.4, 113.2, 110.4, 41.6, 15.3. FT-IR (ATR, cm^{-1}): 3104, 1647, 1570, 1551, 1524, 1394, 1279, 1206, 1184, 1007, 806, 726, 644. ESI-TOF HRMS for $C_{19}H_{17}BrNO$ calculated: 354.0488, found: $[M + H]^+$ 354.0486.

4.2.1.3. **Compound 1c**. The product was obtained as a yellow solid in 87% yield. Melting point: 132–133 °C. ^{1}H-NMR (400.16 MHz, $CDCl_3$, δ/ppm): 8.12 (d, *J* = 15.4 Hz, 1H), 8.04 – 7.98 (m, 1H), 7.88 (dd, *J* = 3.8, 1.2 Hz, 1H), 7.63 (dd, *J* = 5.0, 1.1 Hz, 1H), 7.53 (s, 1H), 7.48 – 7.37 (m, 2H), 7.36 – 7.29 (m, 2H), 7.18 (dd, *J* = 4.9, 3.7 Hz, 1H), 4.19 (q, *J* = 7.3 Hz, 2H), 1.51 (t, *J* = 7.3 Hz, 3H). ^{13}C-NMR (100.63 MHz, $CDCl_3$, δ/ppm): 182.4, 146.5, 138.0, 137.4, 133.0, 132.7, 130.8, 128.1, 126.4, 123.1, 121.6, 120.9, 116.5, 113.0, 110.3, 41.5, 15.2. FT-IR (ATR, cm^{-1}): 3096, 1640, 1562, 1509, 1412, 1273, 1207, 1179, 981, 814, 709, 634. ESI-TOF HRMS for $C_{17}H_{16}NOS$ calculated: 282.0947, found: $[M + H]^+$ 282.0947.

*4.2.2. General procedure for 1,3-diaryl-4-nitrobutan-1-ones (**2a–c**)*

The α,β-unsaturated ketone **1a–c** (1 equivalent, 6.55 mmol) was dissolved in a mixture of methanol/triethylamine (3:2 v/v, 30 mL) and treated with nitromethane (5 equivalents, 32.75 mmol). The reaction mixture was refluxed for 24 hours. After cooling to room temperature, the solvent was removed in vacuo and the residue was dissolved in dichloromethane and washed with a 0.5 M solution of aqueous HCl. The combined organic layers were washed with water, dried over sodium sulfate and concentrated *in vacuo*. The products were purified through column chromatography on silica gel using a mixture of *n*-hexane/acetone as eluting system.

4.2.2.1. **Compound 2a**. The product was obtained as a yellowish oil in 85% yield. ^{1}H-NMR (400.16 MHz, $CDCl_3$, δ/ppm): 7.92 – 7.86 (m, 2H), 7.65 – 7.60 (m, 1H), 7.32 – 7.28 (m, 1H), 7.24 – 7.18 (m, 1H), 7.15 – 7.09 (m, 1H), 7.02 (s, 1H), 6.91 – 6.85 (m, 2H), 4.92 – 4.78 (m, 2H), 4.50 (p, *J* = 6.8 Hz, 1H), 4.07 (q, *J* = 7.3 Hz, 2H), 3.82 (s, 3H), 3.57 – 3.44 (m, 2H), 1.39 (t, *J* = 7.3 Hz, 3H). ^{13}C-NMR (100.63 MHz, $CDCl_3$, δ/ppm): 196.2, 163.8, 136.2, 130.4, 129.7, 126.5, 125.1, 121.9, 119.4, 118.7, 113.9, 112.4, 109.8, 79.2, 55.5, 41.0, 40.8, 31.7, 15.4. FT-IR (ATR, cm^{-1}): 3051, 2974, 2934, 1672,

1547, 1376, 1212, 1166, 1016, 816, 734. ESI-TOF HRMS for $C_{21}H_{23}N_2O_4$ calculated: 367.1652, found: $[M + H]^+$ 367.1653.

4.2.2.2. **Compound 2b**. The product was obtained as a yellowish oil in 80% yield. ^{1}H-NMR (400.16 MHz, $CDCl_3$, δ/ppm): 7.79 – 7.76 (m, 2H), 7.64 – 7.60 (m, 1H), 7.59 – 7.56 (m, 2H), 7.34 – 7.31 (m, 1H), 7.26 – 7.21 (m, 1H), 7.14 (ddd, *J* = 8.0, 7.0, 1.1 Hz, 1H), 7.02 (s, 1H), 4.92 – 4.81 (m, 2H), 4.50 (p, *J* = 7.0 Hz, 1H), 4.11 (q, *J* = 7.3 Hz, 2H), 3.61 – 3.48 (m, 2H), 1.42 (t, *J* = 7.3 Hz, 3H). ^{13}C-NMR (100.63 MHz, $CDCl_3$, δ/ppm): 196.8, 136.3, 135.4, 132.1, 129.7, 128.7, 126.4, 125.1, 122.1, 119.6, 118.7, 112.0, 109.9, 79.1, 41.2, 41.1, 31.6, 15.4. FT-IR (ATR, cm^{-1}): 3054, 2974, 2925, 1682, 1546, 1374, 1206, 1069, 813, 737. ESI-TOF HRMS for $C_{20}H_{20}BrN_2O_3$ calculated: 415.0651, found: $[M + H]^+$ 415.0655.

4.2.2.3. **Compound 2c**. The product was obtained as a yellowish oil in 83% yield. ^{1}H-NMR (400.16 MHz, $CDCl_3$, δ/ppm): 7.70 – 7.60 (m, 3H), 7.35 – 7.31 (m, 1H), 7.25 – 7.21 (m, 1H), 7.18 – 7.12 (m, 1H), 7.11 – 7.07 (m, 1H), 7.05 (s, 1H), 4.95 – 4.82 (m, 2H), 4.52 (p, *J* = 6.9 Hz, 1H), 4.10 (q, *J* = 7.3 Hz, 2H), 3.54 – 3.48 (m, 2H), 1.41 (t, *J* = 7.3 Hz, 3H). ^{13}C-NMR (100.63 MHz, $CDCl_3$, δ/ppm): 190.6, 143.9, 136.2, 134.2, 132.3, 128.3, 126.4, 125.2, 122.0, 119.5, 118.7, 111.9, 109.9, 79.0, 41.8, 41.0, 31.9, 15.4. FT-IR (ATR, cm^{-1}): 3073, 2965, 2935, 1671, 1548, 1374, 1257, 1167, 1023, 828, 699. ESI-TOF HRMS for $C_{18}H_{19}N_2O_3S$ calculated: 343.1110, found: $[M + H]^+$ 343.1108.

*4.2.3. General procedure for the preparation of aza-dipyrromethenes (**3a–c**)*

A mixture of the corresponding 1,3-diaryl-4-nitrobutan-1-ones **2a–c** (1 equivalent, 2.33 mmol) and ammonium acetate (30 equivalents, 69.89 mmol) in butanol (15 mL) was refluxed overnight. After cooling to room temperature and concentration to 2 mL, the precipitate was filtered and washed with methanol. The products were purified through column chromatography on silica gel using dichloromethane as eluent.

4.2.3.1. **Compound 3a**. The product was obtained as a dark blue-black solid in 34% yield. Melting point: >300 °C. ^{1}H-NMR (400.16 MHz, CD_2Cl_2, δ/ppm): 8.11 (d, *J* = 7.8 Hz, 2H), 8.01 – 7.96 (m, 4H), 7.88 (s, 2H), 7.43 (d, *J* = 8.1 Hz, 2H), 7.31 – 7.26 (m, 2H), 7.23 – 7.19 (m, 2H), 7.18 (s, 2H), 7.12 – 7.08 (m, 4H), 4.09 (q, *J* = 7.3 Hz, 4H), 3.92 (s, 6H), 1.37 (t, *J* = 7.3 Hz, 6H). ^{13}C-NMR (100.63 MHz, CD_2Cl_2, δ/ppm): 161.7, 155.1, 150.2, 137.8, 136.9, 130.6, 128.5, 127.8, 126.0, 122.4, 121.5, 120.7, 115.1, 111.4, 110.3, 110.2, 56.0, 41.9, 15.6. FT-IR (ATR, cm^{-1}): 3058, 2928, 1601, 1456, 1244, 1151, 1024, 900, 736. ESI-TOF HRMS for $C_{42}H_{38}N_5O_2$ calculated: 644.3020, found: $[M + H]^+$ 644.3023.

4.2.3.2. **Compound 3b**. The product was obtained as a dark blue-black solid in 25% yield. Melting point: >300 °C. ^{1}H-NMR (400.16 MHz, CD_2Cl_2, δ/ppm): 8.11 – 8.07 (m, 2H), 7.90 – 7.86 (m, 6H), 7.72 – 7.68 (m, 4H), 7.45 – 7.42 (m, 2H), 7.32 – 7.27 (m, 2H), 7.24 – 7.19 (m, 4H), 4.09 (q, *J* = 7.3 Hz, 4H), 1.37 (t, *J* = 7.3 Hz, 6H). ^{13}C-NMR (100.63 MHz, CD_2Cl_2, δ/ppm): 153.5, 150.2, 143.9, 142.9, 132.8, 130.9, 130.4, 128.4, 128.2, 127.7, 122.6, 121.4, 121.0, 111.9, 110.4, 110.1, 42.0, 15.6. FT-IR (ATR,

cm^{-1}): 3059, 2921, 1588, 1531, 1453, 1233, 1006, 901, 788, 732. ESI-TOF HRMS for $C_{40}H_{32}Br_2N_5$ calculated: 740.1018, found: $[M + H]^+$ 740.1016.

4.2.3.3. **Compound 3c**. The product was obtained as a dark blue-black solid in 28% yield. Melting point: >300 °C. ^{1}H-NMR (400.16 MHz, CD_2Cl_2, δ/ppm: 8.08 (d, *J* = 7.9 Hz, 2H), 7.88 (s, 2H), 7.70 – 7.66 (m, 2H), 7.56 – 7.51 (m, 2H), 7.46 – 7.40 (m, 2H), 7.32 – 7.18 (m, 6H), 7.10 (s, 2H), 4.09 (q, *J* = 7.3 Hz, 4H), 1.37 (t, *J* = 7.3 Hz, 6H). ^{13}C-NMR (100.63 MHz, CD_2Cl_2, δ/ppm): 150.2, 150.0, 138.1, 137.9, 136.9, 130.7, 129.2, 128.7, 127.7, 127.3, 122.5, 121.4, 120.9, 111.8, 110.4, 110.0, 41.9, 15.6. FT-IR (ATR, cm^{-1}): 3089, 2973, 1538, 1421, 1380, 1323, 1191, 729, 700. ESI-TOF HRMS for $C_{36}H_{30}N_5S_2$ calculated: 596.1937, found: $[M + H]^+$ 596.1930.

*4.2.4. General procedure for the synthesis of aza-BODIPYs (**4a–c**)*

A solution of the corresponding aza-dipyrromethene **3a–c** (1 equivalent, 0.29 mmol) in dry dichloromethane (20 mL) was treated with triethylamine (2.2 equivalents, 0.64 mmol). The resulting mixture was stirred at room temperature for 10 minutes, followed by addition of $BF_3{\cdot}OEt_2$ (4.4 equivalents, 1.27 mmol). The reaction mixture was refluxed overnight. After cooling to room temperature, the reaction mixture was washed with water. The combined organic layers were washed with brine, dried over sodium sulfate and concentrated *in vacuo*. The products were purified through column chromatography on silica gel using a mixture of *n*-hexane/ dichloromethane as eluting system.

4.2.4.1. **Compound 4a**. The product was obtained as a dark blue-violet solid in yield. Melting point: >300 °C. ^{1}H-NMR (400.16 MHz, CD_2Cl_2, δ/ppm): 8.15 – 8.11 (m, 2H), 8.10 – 8.06 (m, 4H), 8.04 (s, 2H), 7.48 – 7.44 (m, 2H), 7.35 – 7.30 (m, 2H), 7.28 – 7.23 (m, 2H), 7.07 – 7.02 (m, 6H), 4.19 (q, *J* = 7.3 Hz, 4H), 3.90 (s, 6H), 1.46 (t, *J* = 7.3 Hz, 6H). ^{13}C-NMR (100.63 MHz, CD_2Cl_2, δ/ppm): 162.0, 158.0, 145.8, 139.0, 137.2, 132.0, 131.7, 127.6, 125.4, 123.1, 121.6, 121.5, 115.4, 114.4, 110.7, 110.0, 56.0, 42.3, 15.7. ^{19}F-NMR (376.49 MHz, CD_2Cl_2, δ/ppm): -130.11 (q, $J_{(B\text{-}F)}$ = 32.3 Hz). ^{11}B-NMR (128.39 MHz, CD_2Cl_2, δ/ppm): 1.16 (t, $J_{(B\text{-}F)}$ = 32.3 Hz). FT-IR (ATR, cm^{-1}): 3044, 2928, 1601, 1561, 1453, 1433, 1380, 1077, 966, 735. ESI-TOF HRMS for $C_{42}H_{37}BF_2N_5O_2$ calculated: 692. 3002, found: $[M + H]^+$ 692.3003.

4.2.4.2. **Compound 4b**. The product was obtained as a dark blue-violet solid in 79% yield. Melting point: >300 °C. ^{1}H-NMR (400.16 MHz, CD_2Cl_2, δ/ppm): 8.14 – 8.10 (m, 2H), 8.06 (s, 2H), 7.96 – 7.91 (m, 4H), 7.66 – 7.62 (m, 4H), 7.49 – 7.45 (m, 2H), 7.36 – 7.24 (m, 4H), 7.02 (s, 2H), 4.20 (q, *J* = 7.3 Hz, 4H), 1.46 (t, *J* = 7.3 Hz, 6H). ^{13}C-NMR (100.63 MHz, CD_2Cl_2, δ/ppm): 157.6, 140.1, 137.3, 132.5, 132.1, 131.9, 131.4, 128.4, 127.5, 125.2, 123.4, 121.9, 121.5, 115.4, 110.9, 110.2, 42.4, 15.6. ^{19}F-NMR (376.49 MHz, CD_2Cl_2, δ/ppm): -129.44 (q, $J_{(B\text{-}F)}$ = 31.9 Hz). ^{11}B-NMR (128.39 MHz, CD_2Cl_2, δ/ppm): 1.00 (t, $J_{(B\text{-}F)}$ = 31.9 Hz). FT-IR (ATR, cm^{-1}): 3047, 2973, 1570, 1509, 1453, 1425, 1371, 1196, 1003, 798, 737. ESI-TOF HRMS for $C_{40}H_{30}BBr_2F_2N_5$ calculated: 787.0929, found: $[M]^+$ 787.0921.

4.2.4.3. **Compound 4c**. The product was obtained as a dark blue-violet solid in 88% yield. Melting point: >300 °C. ^{1}H-NMR (400 MHz, $CDCl_3$, δ/ppm): 8.32 (dd, *J* = 3.9, 1.0 Hz, 2H), 8.15 – 8.10 (m, 2H), 8.04 (s, 2H), 7.64 (dd, *J* = 5.0, 1.0 Hz, 2H), 7.49 – 7.43 (m, 2H), 7.35 – 7.24 (m, 6H), 7.21 (s, 2H), 4.18 (q, *J* = 7.3 Hz, 4H), 1.45 (t, *J* = 7.3 Hz, 6H). ^{13}C-NMR (101 MHz, $CDCl_3$, δ/ppm): 149.7, 146.1, 138.6, 137.2, 135.1, 132.4, 132.1, 130.9, 129.8, 127.5, 123.2, 121.7, 121.5, 115.2, 110.8, 109.7, 42.3, 15.6. ^{19}F-NMR (376.49 MHz, CD_2Cl_2, δ/ppm): -135.82 (q, $J_{(B-F)}$ = 32.4 Hz). ^{11}B-NMR (128.39 MHz, CD_2Cl_2, δ/ppm): 1.27 (t, $J_{(B-F)}$ = 32.4 Hz). FT-IR (ATR, cm^{-1}): 3088, 2971, 1565, 1504, 1455, 1380, 1133, 1035, 979, 845, 703. ESI-TOF HRMS for $C_{36}H_{29}BF_2N_5S_2$ calculated: 644.1920, found: $[M + H]^+$ 644.1923.

Declaration of interests

The authors declare that they have no known competing financial interests or personal relationships that could have appeared to influence the work reported in this paper.

Acknowledgements

L. L. thanks CONACYT for the grant (576732) supporting his doctoral studies. The authors acknowledge the financial support from CONACYT, PAIP, PAPIIT (IN 222819), and the French-Mexican International Laboratory (LIA-LCMMC-CONACYT) programs.

References and notes

[1] J. V. Frangioni. *Curr. Opin. Chem. Biol*. **2003**, 7, 626.
[2] S-Y. Chang, P. Cheng, G. Li, and Y. Yang. *Joule*. **2018**, 2, 1039.
[3] (a) J. Cure, K. Cocq, A. Nicollet, K. Tan, T. Hungria, S. Assié-Souleille, S. Vivies, L. Salvagnac, M. Quevedo-Lopez, V. Maraval, R. Chauvin, A. Estève, and C. Rossi. *Adv. Sustainable Syst*. **2020**, 4, 2000121; (b) H. Assi, K. Cocq, J. Cure, G. Casterou, K. Castello Lux, V. Collière, L. Vendier, P. Fau, V. Maraval, K. Fajerwerg, Y. J. Chabal, R. Chauvin, and M. L. Kahn. *Int. J. Hydrogen Energy*. **2020**, 45, 24765.
[4] A. Loudet, and K. Burgess. *Chem. Rev*. **2007**, 107, 4891.
[5] (a) J. Murtagh, D. O. Frimannsson, and D. F. O'Shea. *Org. Lett*. **2009**, 11, 5386; (b) M. Tasior, J. Murtagh, D. O. Frimannsson, S. O. McDonnell, and D. F. O'Shea. *Org. Biomol. Chem*. **2010**, 8, 522; (c) A. Palma, L. A. Alvarez, D. Scholz, D. O. Frimannsson, M. Grossi, S. J. Quinn, and D. F. O'Shea. *J. Am. Chem. Soc*. **2011**, 133, 19618; (d) D. Wu, and D. F. O'Shea. *Org. Lett*. **2013**, 15, 3392; (e) L. Bai, P. Sun, Y. Liu, H. Zhang, W. Hu, W. Zhang, Z. Liu, Q. Fan, L. Li, and W. Huang. *Chem. Commun*. **2019**, 55, 10920.
[6] (a) J. Killoran, L. Allen, J. F. Gallagher, W. M. Gallagher, and D. F. O'Shea. *Chem. Commun*. **2002**, 1862; (b) S. O. McDonnell, M. J. Hall, L. T. Allen, A. Byrne, W. M. Gallagher, and D. F. O'Shea. *J. Am. Chem. Soc*. **2005**, 127, 16360; (c) W. M. Gallagher, L. T. Allen, C. O'Shea, T. Kenna, M. Hall, A. Gorman, J. Killoran, and D. F. O'Shea. *Br. J. Cancer*. **2005**, 92, 1702; (d) N. Adarsh, R. R. Avirah, and D. Ramaiah. *Org. Lett*. **2010**, 12, 5720; (e) Y. Gawale, N. Adarsh, S. K. Kalva, J. Joseph, M. Pramanik, D. Ramaiah, and N. Sekar. *Chem. Eur. J*. **2017**, 23, 6570.
[7] (a) M. J. Hall, L. T. Allen, and D. F. O'Shea. *Org. Biomol. Chem*. **2006**, 4, 776; (b) A. Coskun, M. D. Yilmaz, and E. U. Akkaya. *Org. Lett*. **2007**, 9, 607; (c) R. E. Gawley, H. Mao, M. M. Haque, J. B. Thorne, and J. S. Pharr. *J. Org. Chem*. **2007**, 72, 2187; (d) S. Liu, Z. Shi, W. Xu, H. Yang, N. Xi, X. Liu, Q. Zhao, and W. Huang. *Dyes Pigm*.

2014, 103, 145; (e) H-J. Xiang, H. P. Tham, M. D. Nguyen, S. Z. Fiona-Phua, W. Q. Lim, J-G. Liu, and Y. Zhao. *Chem. Commun*. **2017**, 53, 5220.
[8] (a) T. Mueller, R. Gresser, K. Leo, and M. Riede. *Sol. Energy Mater. Sol. Cells*. **2012**, 99, 176; (b) J. Min, T. Ameri, R. Gresser, M. Lorenz-Rothe, D. Baran, A. Troeger, V. Sgobba, K. Leo, M. Riede, D. M. Guldi, and C. J. Brabec. *ACS Appl. Mater. Interfaces*. **2013**, 5, 5609; (c) T. K. Khan, P. Sheokand, and N. Agarwal. *Eur. J. Org. Chem*. **2014**, 1416; (d) S. Kraner, J. Widmer, J. Benduhn, E. Hieckmann, T. Jägeler-Hoheisel, S. Ullbrich, D. Schütze, K. S. Radke, G. Cuniberti, F. Ortmann, M. Lorenz-Rothe, R. Meerheim, D. Spoltore, K. Vandewal, C. Koerner, and K. Leo. *Phys. Status Solidi A*. **2015**. 212, 2747; (e) T-J. Li, T. Meyer, R. Meerheim, M. Höppner, C. Körner, K. Vandewal, O. Zeika, and K. Leo. *J. Mater. Chem. A*. **2017**, 5, 10696.
[9] (a) P-A. Bouit, K. Kamada, P. Feneyrou, G. Berginc, L. Toupet, O. Maury, and C. Andraud. *Adv. Mater*. **2009**, 21, 1151; (b) B. Küçüköz, M. Hayvali, H. Yilmaz, B. Uguz, U. Kürüm, H. G. Yaglioglu, and A. Elmali. *J. Photochem. Photobiol. A*. **2012**, 247, 24; (c) M. Frenette, M. Hatamimoslehabadi, S. Bellinger-Buckley, S. Laoui, S. Bag, O. Dantiste, J. Rochford, and C. Yelleswarapu. *Chem. Phys. Lett.* **2014**, 608, 303; (d) G. Kubheka, O. Achadu, J. Mack, and T. Nyokong. *New J. Chem*. **2017**, 41, 12319; (e) S. Pascal, Q. Bellier, S. David, P-A. Bouit, S-H. Chi, N. S. Makarov, B. Le Guennic, S. Chibani, G. Berginc, P. Feneyrou, D. Jacquemin, J. W. Perry, O. Maury, and C. Andraud. *J. Phys. Chem. C*. **2019**, 123, 23661.
[10] A. Gorman, J. Killoran, C. O'Shea, T. Kenna, W. M. Gallagher, and D. F. O'Shea. *J. Am. Chem. Soc*. **2004**, 126, 10619.
[11] (a) S. O. McDonnell, and D. F. O'Shea. *Org. Lett*. **2006**, 8, 3493; (b) J. Killoran, S. O. McDonnell, J. F. Gallagher, and D. F. O'Shea. *New J. Chem*. **2008**, 32, 483.
[12] L. Jiao, Y. Wu, S. Wang, X. Hu, P. Zhang, C. Yu, K. Cong, Q. Meng, E. Hao, and M. G. H. Vicente. *J. Org. Chem*. **2014**, 79, 1830.
[13] (a) W. Zhao, and E. M. Carreira. *Angew. Chem. Int. Ed*. **2005**, 44, 1677; (b) W. Zhao, and E. M. Carreira. *Chem. Eur. J*. **2006**, 12, 7254; (c) X-D. Jiang, D. Xi, C-L. Sun, J. Guan, M. He, and L-J. Xiao. *Tetrahedron Lett*. **2015**, 56, 4868.
[14] (a) A. Loudet, R. Bandichhor, L. Wu, and K. Burgess. *Tetrahedron*. **2008**, 64, 3642; (b) Q. Bellier, S. Pégaz, C. Aronica, B. Le Guennic, C. Andraud, and O. Maury. *Org. Lett*. **2011**, 13, 22; (c) N. Balsukuri, N. Manav, M. Y. Lone, S. Mori, A. Das, P. Sen, and I. Gupta. *Dyes Pigm*. **2020**, 176, 108249.
[15] (a) V. F. Donyagina, S. Shimizu, N. Kobayashi, and E. A. Lukyanets. *Tetrahedron Lett*. **2008**, 49, 6152; (b) H. Lu, S. Shimizu, J. Mack, Z. Shen, and N. Kobayashi. *Chem. Asian J*. **2011**, 6, 1026; (c) R. Gresser, M. Hummert, H. Hartmann, K. Leo, and M. Riede. *Chem. Eur. J*. **2011**, 17, 2939.
[16] (a) A. Loudet, R. Bandichhor, K. Burgess, A. Palma, S. O. McDonnell, M. J. Hall, and D. F. O'Shea. *Org. Lett*. **2008**, 10, 4771; (b) V. P. Yakubovskyi, M. P. Shandura, and Y. P. Kovtun. *Synth. Commun*. **2010**, 40, 944; (c) Y. Kubo, T. Shimada, K. Maeda, and Y. Hashimoto. *New J. Chem*. **2020**, 44, 29.
[17] (a) R. Gresser, H. Hartmann, M. Wrackmeyer, K. Leo, and M. Riede. *Tetrahedron*. **2011**, 67, 7148; (b) X. Zhang, H. Yu, and Y. Xiao. *J. Org. Chem*. **2012**, 77, 669; (c) Q. Bellier, F. Dalier, E. Jeanneau, O. Maury, and C. Andraud. *New J. Chem*. **2012**, 36, 768.
[18] (a) F. Bureš. *RSC Adv*. **2014**, 4, 58826; (b) Z. Tang, X. Sun, and P. Zhang. *Adv. Mater. Res*. **2014**, 1061, 291.
[19] (a) N. Balsukuri, M. Y. Lone, P. C. Jha, S. Mori, and I. Gupta. *Chem. Asian J*. **2016**, 11, 1572; (b) N. Balsukuri, N. J. Boruah, P. E. Kesavan, and I. Gupta. *New J. Chem*. **2018**, 42, 5875.
[20] J. Kumar, N. Kumar, and P. K. Hota. *RSC Adv*. **2020**, 10, 28213.
[21] R. Jiang, X. Yang, and D. Wu. *Org. Biomol. Chem*. **2017**, 15, 6888.
[22] (a) S. O. Mcdonnell, and D. F. O'Shea. *Org. Lett*. **2006**, 8, 3493; (b) A. Loudet, R. Bandichhor, K. Burgess, A. Palma, S. O. McDonnell, M. J. Hall, and D. F. O'Shea. *Org. Lett*. **2008**, 10, 4771.
[23] C. Reichardt. *Solvents and Solvent Effects in Organic Chemistry*, 3rd ed, chap. 7, pp 389–469, Wiley-VCH, **2003**.
[24] (a) B. Le Guennic, O. Maury, and D. Jacquemin. *Phys. Chem. Chem. Phys*. **2012**, 14, 157; (b) S. Chibani, B. Le Guennic, A. Charaf-Eddin, O. Maury, C. Andraud, and D. Jacquemin. *J. Chem. Theory Comput*. **2012**, 8, 3303; (c) S. Chibani, B. Le Guennic, A. Charaf-Eddin, A. D. Laurent, and D. Jacquemin. *Chem. Sci*. **2013**, 4, 1950; (d) A. Gut, Ł. Łapok, D. Jamróz, and M. Nowakowska. *Asian J. Org. Chem*. **2017**, 6, 207.
[25] M. J. Frisch, G. W. Trucks, H. B. Schlegel, G. E. Scuseria, M. A. Robb, J. R. Cheeseman, G. Scalmani, V. Barone, B. Mennucci, G. A. Petersson, H. Nakatsuji, M. Caricato, X. Li, H. P. Hratchian, A. F. Izmaylov, J.

Bloino, G. Zheng, J. L. Sonnenberg, M. Hada, M. Ehara, K. Toyota, R. Fukuda, J. Hasegawa, M. Ishida, T. Nakajima, Y. Honda, O. Kitao, H. Nakai, T. Vreven, J. A. Montgomery, Jr., J. E. Peralta, F. Ogliaro, M. Bearpark, J. J. Heyd, E. Brothers, K. N. Kudin, V. N. Staroverov, T. Keith, R. Kobayashi, J. Normand, K. Raghavachari, A. Rendell, J. C. Burant, S. S. Iyengar, J. Tomasi, M. Cossi, N. Rega, J. M. Millam, M. Klene, J. E. Knox, J. B. Cross, V. Bakken, C. Adamo, J. Jaramillo, R. Gomperts, R. E. Stratmann, O. Yazyev, A. J. Austin, R. Cammi, C. Pomelli, J. W. Ochterski, R. L. Martin, K. Morokuma, V. G. Zakrzewski, G. A. Voth, P. Salvador, J. J. Dannenberg, S. Dapprich, A. D. Daniels, O. Farkas, J. B. Foresman, J. V. Ortiz, J. Cioslowski, and D. J. Fox. *Gaussian 09*, *Revision D.01*, Gaussian, Inc., Wallingford CT, 2013.

[26] For regrading the concept of π-frustation and exemplification with 1-ethyl-indol-3-yl substituents see: (a) A. Rives, I. Baglai, V. Malytskyi, V. Maraval, N. Saffon-Merceron, Z. Voitenko, and R. Chauvin. *Chem. Commun*. **2012**, 48, 8763; (b) I. Baglai, V. Maraval, C. Bijani, N. Saffon-Merceron, Z. Voitenko, Y. M. Volovenko, and R. Chauvin. *Chem. Commun*. **2013**, 49, 8374; (c) I. Baglai, V. Maraval, Z. Voitenko, Y. Volovenko, and R. Chauvin. *Fr. Ukr. J. Chem*. **2013**, 1, 48.

[27] Q. K. Sun, W. Liu, S. A. Ying, L. L. Wang, S. F. Xue, and W. J. Yang. *RSC Adv*. **2015**, 5, 73046.

Graphical abstract